

Experiments on active control of structurally radiated sound using multiple piezoceramic actuators

Robert L. Clark and Chris R. Fuller

Mechanical Engineering Department, Virginia Polytechnic Institute and State University, Blacksburg, Virginia 24061

(Received 7 December 1990; revised 16 September 1991; accepted 12 February 1992)

Active control of sound radiation from a vibrating rectangular plate excited by a steady-state harmonic point force disturbance is experimentally studied. Control structural inputs are achieved by three piezoceramic actuators bonded to the surface of the panel. Microphones were implemented as error sensors in the radiated field, while the control approach was based upon a filtered-X version of the adaptive least-mean-squares (lms) algorithm. Both position and number of piezoceramic actuators were varied during the test to determine the effects on control authority. A variety of test cases were studied for controlling sound radiation due to a disturbance both on and off resonance. Results from these experiments indicate that piezoceramic elements provide an efficient method for distributed modification of structural response to attenuate sound radiation. In addition, the adaptive lms algorithm is shown to be an effective narrow-band controller, which in contrast to feedback approaches, requires little system modeling.

PACS numbers: 43.40.Dx, 43.40.Vn

INTRODUCTION

Much research has been devoted to the study of adaptive control of structures in an effort to reduce the far-field sound radiation. Recent work has been devoted to the implementation of point force inputs to control sound radiation from plate structures.¹⁻³ In addition to the fact that point force inputs can sometimes lead to "control spillover," physical limitations are imposed due to the nature of the hardware necessary in implementing the control (i.e., shakers capable of providing the necessary control must be physically attached to the structure and often require additional reaction mounting). Recent analytical studies have suggested a piezoelectric actuator as an alternative control input in order to overcome some of these disadvantages.⁴⁻⁷

Piezoelectric actuators can be bonded directly to the structural surface or embedded in the material, becoming an integral part of the system. At this point, the structure can be labeled an adaptive structure since the actuators enable the alteration of system states or characteristics in a controlled manner.⁸ Crawley and de Luis,⁴ Bailey and Hubbard,⁵ and Fanson and Chen⁶ have all investigated structural control with the use of piezoelectric actuators. Recent analytical studies have been devoted to controlling sound radiation from flat plates with piezoelectric actuators.^{7,9} In addition, Fuller *et al.* experimentally studied the control of sound radiation from a simply supported rectangular plate with a single piezoelectric actuator as the control input.¹⁰ In that study, control of far-field sound was achieved by "modal suppression," meaning that during control, all of the modal amplitudes were reduced. The alternative to modal suppression is "modal restructuring." In modal restructuring, the modal amplitudes can increase; however, the residual structural response has a lower overall radiation efficiency leading to a reduction in far-field sound levels.¹¹

As an extension to the work conducted by Fuller *et al.*,¹⁰

the present study considers distributed control of the structure, utilizing up to three piezoelectric actuators as control inputs, in conjunction with an advanced adaptive controller. In the present work, the control approach was based upon a filtered-X version of the adaptive least-mean-squares (lms) algorithm, and microphones located in the radiated field were implemented as error sensors. In conducting the tests, a variety of cases were studied for controlling sound radiation due to a disturbance both on and off resonance. In addition, the number of control channels and position of control actuators were varied to illustrate the advantages of distributed control. Based on results of these experiments, piezoelectric actuators are demonstrated to provide an efficient method for distributed control of structural response to attenuate sound radiation. In addition, the adaptive lms algorithm is shown to be an effective narrow-band controller, which in contrast to feedback approaches, requires a much *lower* degree of system modeling.

I. EXPERIMENTAL SETUP

Experiments were performed in the anechoic chamber at Virginia Polytechnic Institute and State University which has dimensions $4.2 \times 2.2 \times 2.5$ m and a cutoff frequency of 250 Hz. The test plate, which was mounted in a rigid steel frame, was cut from steel and measured $380 \times 300 \times 1.96$ mm. The simply supported boundary conditions were achieved by attaching thin shim spring steel to the boundaries of the plate with small set screws and a sealing compound. The shims were then attached to the rigid steel frame, allowing the plate to bend relatively freely but restricting out of plane motion at the boundaries. Previous testing has shown that this arrangement adequately models the simply supported boundary conditions.¹² The test rig was placed in the anechoic chamber where it was rigidly supported on a structure configured with a $4.2\text{-m} \times 2.2\text{-m} \times 19\text{-mm}$ wooden

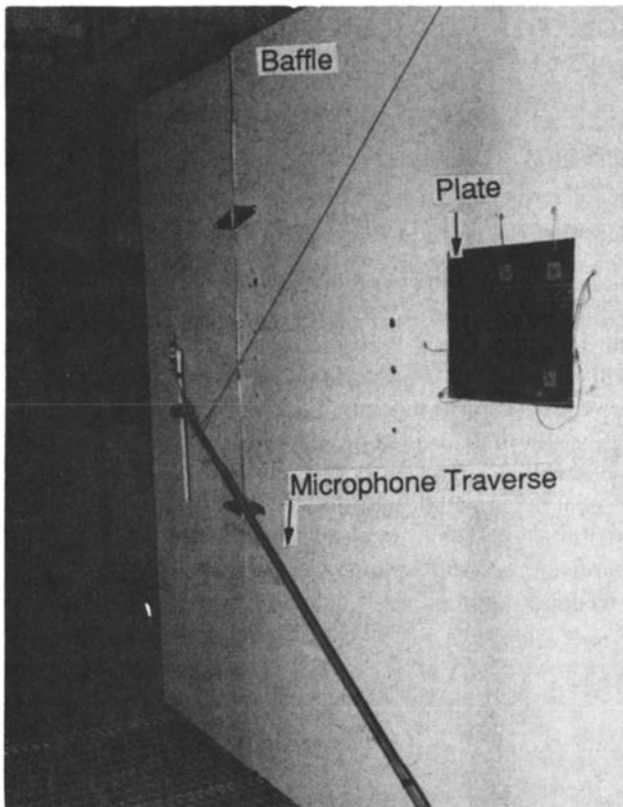


FIG. 1. Experimental arrangement.

baffle. The baffle was implemented to reduce the dipole effect created by the front and back of the plate as well as facilitate later analytical comparisons. As illustrated in Fig. 1, the plate resides in the center of the baffle.

For the noise input, the plate was driven with a shaker attached to the back of the structure with a stinger at spatial coordinates of (240, 130 mm) from the left lower corner of the front of the plate. The plate was instrumented with nine Bruel & Kjaer mini accelerometers, weighing less than 0.65 g each, and the output of these accelerometers was analyzed by solving a set of simultaneous equations to recover the amplitudes of independent modes on the panel.³ This method is further discussed in the Appendix. The directivity pattern was obtained by traversing the acoustic field with a Bruel & Kjaer microphone. Acoustic measurements were obtained in 9° increments about the horizontal midplane of the plate at a radius of 1.6 m. For the frequency range of interest, this radius was not at a coordinate location where the far-field relations could be accurately used; however, this was the greatest radius possible due to the finite dimensions of the chamber. The sound radiation directivity pattern was mapped both with and without control. In addition, a few microphones were randomly located in the chamber to provide a measure of the global attenuation. The output of all transducers was sampled and signal processed with a model 2032 Bruel & Kjaer spectrum analyzer.

Two identical plates were constructed for testing; however, the positions of the piezoceramic actuators were varied to illustrate the effect on distributed control. The first plate was configured with three sets of piezoelectric actuators as

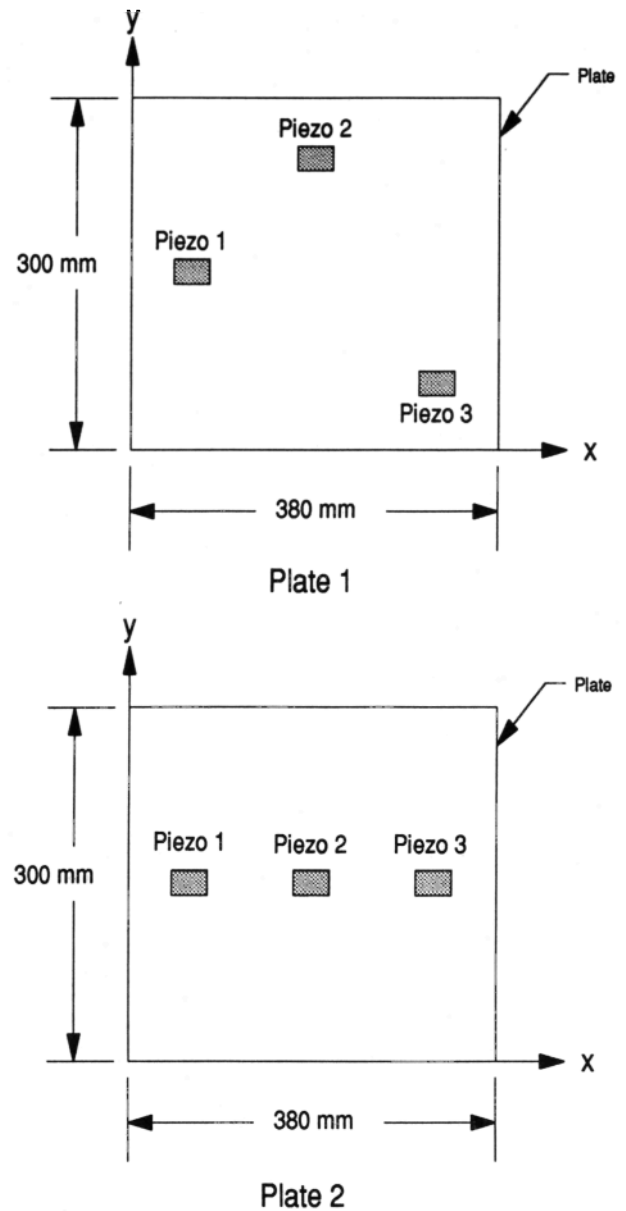


FIG. 2. Schematic of plates 1 and 2.

illustrated in Fig. 2. The center of each of the three actuators was located at spatial coordinates of (63.3, 150 mm), (190, 250 mm), and (316.6, 50 mm), respectively. Notice that the orientation of actuators allows coupling with odd modes (shown in Fig. 3) in the y direction as well as those in the x direction. Each actuator consists of two piezoceramic elements of dimensions $38.1 \times 21 \times 0.19$ mm bonded symmetrically (front and back). The actuator material was PZT G-1195 supplied by Piezoelectric Products Incorporated. The second plate was also configured with three sets of piezoelectric actuators with orientation as depicted in Fig. 2. The center of each of the three actuators was located at spatial coordinates of (63.3, 150 mm), (190, 150 mm), and (316.6, 150 mm), respectively. Notice that the actuators are optimally positioned to couple with the (3,1) mode of the plate (i.e., at the antinodes where surface strain is the highest for this mode).

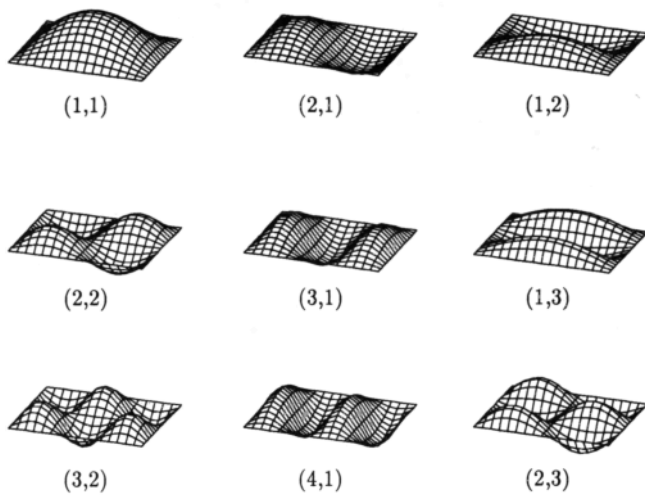


FIG. 3. Schematic of mode shapes (m,n) .

All piezoelectric elements were bonded to the structure with M-bond 200 adhesive, and the glue layer was maintained as thin as possible (approximately 0.02 mm). A thin foil lead (approximately 0.01 mm) was soldered to the underside of the piezoelectric patch, and a wire was soldered directly to the exposed side of the patch to complete the electrical circuit necessary to drive the element. The symmetrically located patches were wired out of phase such that a voltage inducing extension on one side of the plate would induce contraction on the opposite, resulting in uniform bending about the neutral axis of the plate. With this configuration, driving the actuators electrically results in line moments acting around the boundaries of the actuator as discussed by Dimitriadis *et al.*¹³

A modal analysis of each of the previously described plates was performed to extract the resonant frequencies and compare them to those computed from thin plate theory. As evident in the results presented in Table I, the measured resonant frequencies are within 1% for the modes presented. For future reference, a schematic of the mode shapes for a simply supported plate is presented in Fig. 3.

A signal generator was used to create a harmonic disturbance and the signal was amplified to drive the shaker. The same signal was input as the reference of the controller. The control outputs from the digital to analog board were amplified separately. To obtain the necessary high voltage re-

TABLE I. Theoretical versus experimental resonant frequencies.

Mode	Theoretical f_{mn} (Hz)	Experimental f_{mn} (Hz)
(1,1)	88	88
(2,1)	189	187
(1,2)	250	253
(2,2)	351	349
(3,1)	357	353
(1,3)	519	511
(3,2)	520	522
(4,1)	592	584
(2,3)	621	612

quired by the piezoelectric actuators, a 17:1 voltage transformer was used to increase the amplifier output voltage. Due to the high impedance of the PZT, the input voltage could not be measured directly; however, it was measured on the input side of the transformer to assure that the actuators were not over driven (i.e., less than ≈ 180 Vrms).¹⁴

II. DESCRIPTION OF CONTROLLER

To achieve control, a three-channel adaptive controller based on the multichannel version of the Widrow-Hoff filtered-X control algorithm was implemented on a TMS320C25 DSP resident in an AT computer. This algorithm is described in detail by Elliott *et al.*¹⁵ A block diagram illustrating the control system is presented in Fig. 4. The output of an error sensor can be modeled at the n th time step as

$$e_l(n) = d_l(n) + \sum_{m=1}^M \sum_{j=0}^{N-1} P_{lmj} \sum_{i=0}^{N-1} w_{mi}(n-j)x(n-i-j), \quad (1)$$

where $d_l(n)$ is the l th error sensor, $x(n)$ is the input reference source, w_{mi} are the coefficients of the adaptive finite impulse response (FIR) filters, and P_{lmj} is the j th coefficient of the transfer function between the output of the m th adaptive filter and the l th error sensor. The number of control actuators and filter coefficients are designated by M and N , respectively.

In the lms algorithm, the mean-square-error signal is defined by

$$J = E \left(\sum_{l=1}^L e_l^2(n) \right), \quad (2)$$

where E is the expectation operator. Since this error function is quadratic, only one minimum solution exists. The outputs of the fixed filters, \hat{P}_{lmj} , at each time step n , were used by the lms algorithm to minimize the mean-square-error signal by modifying the coefficients of the adaptive filter as follows:

$$w_{mi}(n+1) = w_{mi}(n) - \mu \sum_{l=1}^L e_l(n) r_{lm}(n-i), \quad (3)$$

where

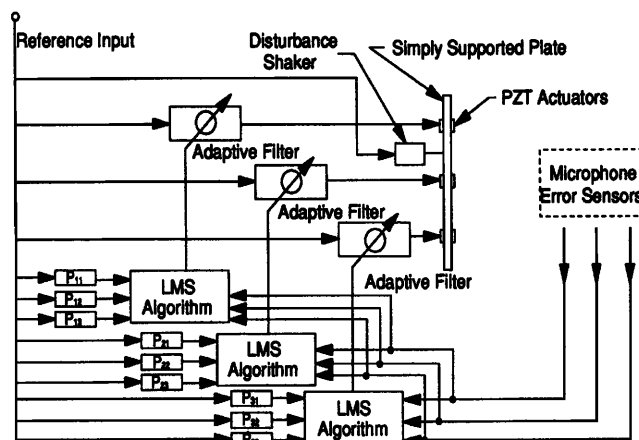


FIG. 4. Block diagram of controller.

$$r_{lm}(n-i) = \sum_{j=0}^{N-1} \hat{P}_{lmj} x(n-i-j). \quad (4)$$

Note that the summation in Eq. (3) is an estimate of the gradient necessary in updating the weighting coefficients. As opposed to taking the expectation of the error signal as indicated in Eq. (2), the square of the error signal is simply taken as an estimate of the desired expectation in the lms algorithm. As a result, the gradient components contain a large contribution of noise; however, the noise is attenuated with time due to the adaptive process.¹⁶ In Eq. (3), L is the total number of error sensors utilized and $L \geq M$. The coefficients $r_{lm}(n)$ are the outputs of the compensating filters \hat{P}_{lmj} which are estimates of the actual coefficients, P_{lmj} measured prior to starting the control algorithm. This procedure is necessary since the lms algorithm assumes that the error $e_l(n)$ is the instantaneous result of the control input for which the signal $r_{lmn}(n)$ is a better estimate than $x(n)$ (Ref. 15). The factor μ in Eq. (3) is the gain constant that regulates the speed and stability of convergence.

A steady-state sinusoid was used as the disturbance signal for all tests conducted. A signal generator resident on the Bruel & Kjaer model 2032 spectrum analyzer was used to create the disturbance and reference signal for the lms controller. Since the signal was sinusoidal, a finite impulse response filter with two coefficients can be implemented to modify the phase and magnitude of the signal. While a narrow-band controller was utilized in the tests, multiple channels were implemented in the control algorithm, up to three as illustrated in Fig. 4. The choice of sampling rate was based upon the frequency of the disturbance since low-frequency signals require slower sampling rates for stable convergence.

III. EXPERIMENTAL PROCEDURE

Experiments were conducted for both on and off resonance cases of the plates. Identical tests were performed on both plates such that results could readily be compared. In outlining the test procedures, only one plate will be discussed, realizing that the test procedures were uniformly applied to both plates.

For the on resonance cases, the panel was tuned for resonant response by driving the shaker near the resonance and varying the frequency while monitoring the response of an accelerometer located at an antinode for the desired mode of the structure. The frequency corresponding to the maximum response was determined to be the resonant frequency. This procedure was performed each day a test was conducted to compensate for changes in resonant response due to slight fluctuations in ambient temperature, which was approximately 25.4 °C. Upon determining the resonant frequency of the (3,1) mode, the plate was driven with the shaker at a level resulting in acoustic radiation ranging from 60 to 80 dB (referenced to 20 μ Pa) at a radius of 1.6 m from the plate.

The test procedure was identical for both the on and off resonance cases. Before applying control, the response of the array of accelerometers was measured and the acoustic field was traversed with a microphone to obtain the resulting directivity pattern. The signals of the accelerometers were used in the modal decomposition algorithm described in the

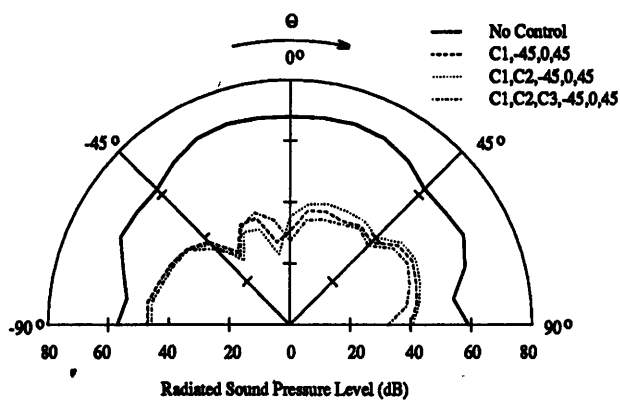
Appendix. After obtaining measurements from the uncontrolled case, the filtered-X lms algorithm was invoked, and the plate was controlled via the piezoelectric actuators. Upon converging to the minimum acoustic response at each microphone, acoustic and structural measurements were obtained. After obtaining these measurements, the uncontrolled and controlled responses were compared for both the acoustic radiation and the structural vibration. Note that the closed loop response of the structure is decomposed into the simply supported or open loop modal amplitudes in order to make direct comparisons. In reality, it has been shown by Burdisso and Fuller¹⁷ that the closed loop system has new resonant frequencies and associated mode shapes similar to feedback control.

IV. RESULTS

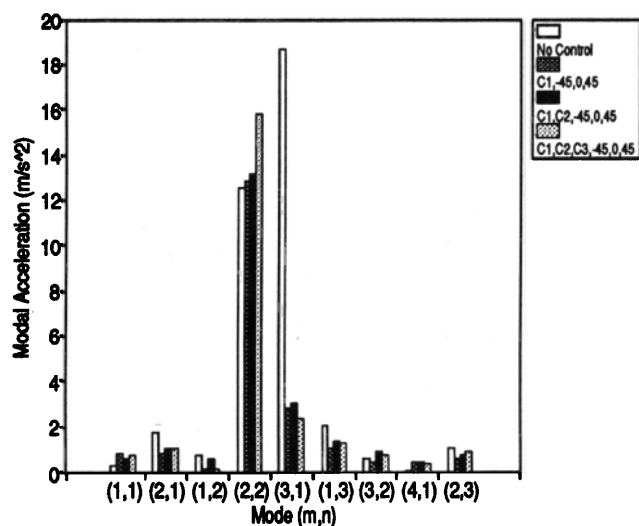
A. Multichannel control comparison

For the first case, plate 1 was driven slightly below resonance of the (3,1) mode at an excitation frequency of 351 Hz. Since the resonant frequency of the (2,2) mode is 349 Hz and the resonant frequency of the (3,1) mode is 353 Hz, contributions from both modes were expected. Both the acoustic response and modal response of the plate are illustrated in Fig. 5(a) and (b), respectively. In the legend of the figure, "C#" indicates the respective piezoelectric actuator used in the control implementation, and the error microphone position is given in units of degrees about the mid-plane of the plate. In this case, microphones located at +45°, 0°, and -45° were implemented as error sensors, while the number of control actuators was varied between one and three. As is obvious from the acoustic response, the radiated sound was attenuated between 30 and 40 dB with little discernible differences while increasing the number of control inputs. The method of control was very similar whether using three control actuators or one as can be seen in Fig. 5(b). Modal reduction appears to be the dominant mechanism in achieving sound attenuation while modal restructuring is also evident as observed with the increase of the amplitude of the (2,2) mode upon achieving control. The modal response of the (1,1) mode was observed to increase as well; however, destructive interference occurred between the (1,1) and (3,1) mode as they were out of phase with respect to each other. The increased response of the (2,2) mode was of little significance since it is an inefficient acoustic radiator. The overall result is a reduction in the radiated sound pressure.

As a second case, plate 1 was driven well off resonance at 400-Hz implementing microphones at the same coordinates as in the previous test case and again increasing the number of control inputs from one to three. The acoustic response and modal response for this test case are presented in Fig. 6(a) and (b), respectively. In contrast to the on resonance case, significant improvement in sound reduction is observed with increasing number of control inputs. While only 5 to 10 dB of noise reduction was obtained when implementing a single channel of control, as much as 30 dB of sound attenuation was achieved when utilizing three control inputs. As the component modal amplitudes and thus overall plate response typically increased under control conditions

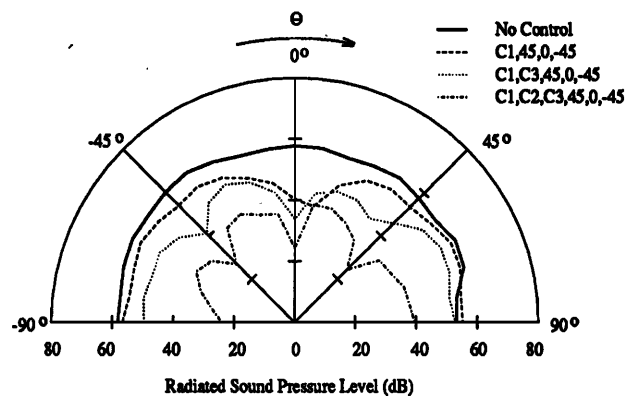


(a) Acoustic Directivity Pattern

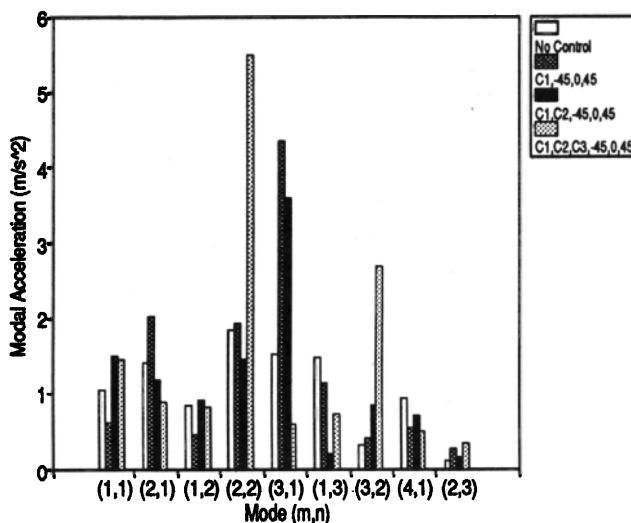


(b) Modal Amplitudes

FIG. 5. Response on-resonance of (3,1) mode (plate 1).



(a) Acoustic Directivity Pattern



(b) Modal Amplitudes

FIG. 6. Response at 400 Hz (plate 1).

attenuation of sound was achieved through modal restructuring. To achieve reduction in sound radiation with increasing plate response, the residual response of the plate must have a lower overall radiation efficiency than the open loop case.

In discussing the advantages of implementing multiple channels for controlling sound radiation from the plate, the two cases previously presented will be considered. The first case presented in Fig. 5 corresponded to the resonant response of the (3,1) mode of the plate. In this experiment, little if any improvement in sound attenuation was observed when increasing the number of control channels. This result was expected since each piezoelectric actuator implemented in the control was observed to couple equally well to the (3,1) mode of the structure, which is dominant in the response as indicated by the modal decomposition. In addition,

the acoustic field is dominated by the (3,1) mode, which is an efficient radiator. As a result, only one control actuator was required to effectively couple to the structural mode creating the undesired noise.

Results from the off resonance case presented in Fig. 6 are quite different. A significant improvement in sound attenuation was observed with increasing number of control inputs, approximately 10 dB per control channel. This can be explained when considering results from the modal decomposition. The structural response is more "modally rich" for the uncontrolled case since multiple modes are necessary to create the disturbance measured at 400 Hz. If only one channel of control is implemented, the phasing of this control input can be varied relative to that of the disturbance to attenuate the undesired noise; however, there is a limit to the possible variations. As the number of control channels

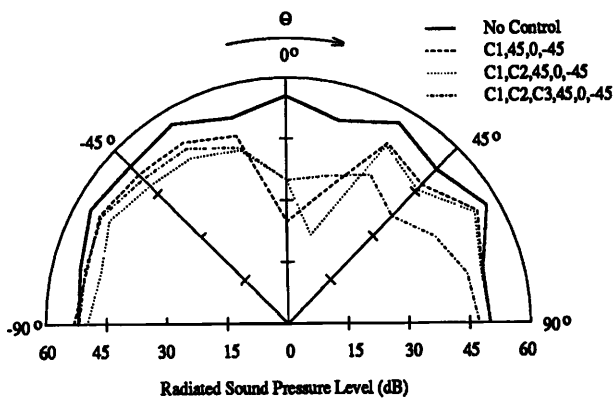
increases, more complex phasing of actuators is possible resulting in distributed control of the panel. In general, as the response of the structure is dominated by multiple modes, a proportional number of actuators is necessary to provide the degrees of freedom necessary in creating the control input, unless of course those modes are inefficient acoustic radiators.

B. Effect of actuator location on distributed control

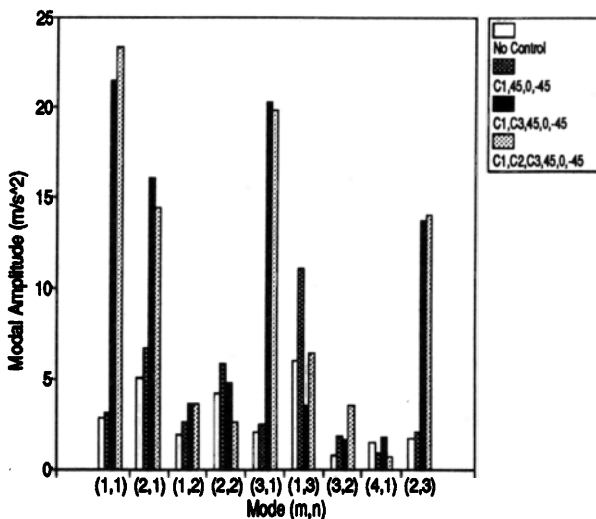
A second plate was constructed primarily for the study of resonance cases, specifically for controlling the (3,1) mode. However, for off resonance cases, control authority with actuators positioned as those on plate 2 was observed to be poor since coupling into odd modes in the y direction of the plate was practically impossible. Placement of actuators on plate 1 were chosen to alleviate this problem. A compar-

son was made between levels of attenuation obtained from plates 1 and 2 at a frequency of 400 Hz. Results from plate 1 were previously presented in Fig. 6. In general, sound attenuation on the order of 30 dB was obtained when implementing three control actuators and error microphones. Results from tests conducted on plate 2 are presented in Fig. 7. While significant attenuation was achieved at the microphone located at 0° , in general, global attenuation was observed to be poor (on the order of 0 to 5 dB). The most significant observation that can be made when comparing the modal amplitudes of Figs. 6 and 7 is that the response of the (1,1) mode is negligible under control conditions for plate 1, while significant in the response of plate 2 under control conditions. This is an undesirable effect under control since this mode is an efficient acoustic radiator (i.e., spillover is occurring into an important mode).

A high level of response of these modes can be attributed to the location of the piezoelectric actuators on plate 2 that are positioned to couple strongly to the (1,1) and (3,1) modes. As the actuators are on the plate horizontal centerline, they cannot strongly couple into modes with vertical symmetric components (theoretically totally decoupled). However, as discussed in the companion paper¹⁸ at around 400 Hz for this geometry of the plate, the (1,2) mode contributes significantly to the radiated energy. Thus the controller attempts, with limited success, to attenuate these radiation components by increasing the response of the (1,1) and (3,1) modes so that the combined structural response has a lower radiation efficiency. When three actuators are located off the midplane, as in plate 1, the control can now be achieved by directly attenuating most of the significant modal contributions and far higher levels of attenuation are achieved. Thus the location of the actuators is extremely important for effective and efficient sound reduction.



(a) Acoustic Directivity Pattern



(b) Modal Amplitudes

FIG. 7. Response at 400 Hz (plate 2).

V. CONCLUSIONS

Active control of sound radiation from a vibrating simply supported rectangular plate excited by a steady-state harmonic point force disturbance has been experimentally studied. For on resonance cases, only marginal improvement in sound attenuation was achieved by increasing the number of control piezoelectric actuators. This result was not surprising since the acoustic response on resonance is usually dominated by one mode of the structure.

For the off resonance cases, the contrary was observed. Increasing the number of control actuators was directly correlated with improvement in sound attenuation. In addition, the position of piezoelectric actuators on the plate was critical to obtaining the desired structural response in order to reduce sound radiation. Since the acoustic response results from a more complex interaction between structural modes for off resonance cases, increasing the number of control actuators provides a method for the controller to create the necessary response by optimally varying the phase and magnitude between actuators. In other words, a higher-order controller has more degrees of freedom in terms of structural response.

Based on results of this study, the adaptive lms algorithm is shown to be an effective narrow-band controller,

which in contrast to feedback approaches, requires a much *lower* degrees of system modeling. The combination of multiple piezoelectric actuators with an adaptive lms algorithm provides the flexibility necessary in minimizing the acoustic radiation of a structure for both on and off resonance disturbances. In general, these trends seen in the experimental investigation agree well with those of an analysis of a similar arrangement.⁷ Future work will be devoted to optimizing the location of the piezoelectric actuators for controlling structure-borne sound radiation. In addition, a companion paper studies the use of PVDF structural error sensors.¹⁸

ACKNOWLEDGMENT

This work was supported by DARPA/ONR under Grant No. ONR-N00014-88-K-0721.

APPENDIX

The modal decomposition follows a method previously outlined by Hansen *et al.*³ For a simply supported plate, the displacement response *w* can be represented as follows:

$$w(x,y,t) = \sum_{m=1}^{\infty} \sum_{n=1}^{\infty} A_{mn} \sin\left(\frac{m\pi x}{L_x}\right) \sin\left(\frac{n\pi y}{L_y}\right) \exp(j\omega t), \tag{A1}$$

where *m* and *n* represent the mode number, *L_x* and *L_y* are the plate dimensions, *ω* is the frequency of vibration, and *A_{mn}* are the modal amplitudes.

Nine accelerometers were randomly placed on the plate, and an additional reference accelerometer was placed on the plate away from nodal lines of modes desired in the decomposition. Since only two channels of A/D were available on the spectrum analyzer, a reference accelerometer was required to obtain phasing of the measurements. The frequency response function between each randomly placed accelerometer and the reference accelerometer was measured as well as the autospectrum of the reference accelerometer. The autospectrum provides a means of scaling the data in terms of engineering units. By computing the frequency response function, phase information is also obtained. If the plate is assumed to respond as predicted in the theoretical analysis, a matrix of spatial coefficients can be generated from the theoretical eigenvectors by substituting the spatial coordinates of the randomly positioned accelerometers into the equation. For nine independent measurements, nine distinct modal amplitudes can be computed, resulting in a 9×9 matrix of the eigenvectors. After measuring the acceleration at each of these coordinates, a system of linear algebraic equations results.

$$[W] = [S][A], \tag{A2}$$

where the matrix of measurement is

$$[W] = \begin{bmatrix} W_1 \\ \cdot \\ \cdot \\ \cdot \\ W_k \end{bmatrix}, \tag{A3}$$

while modal amplitudes are

$$[A] = \begin{bmatrix} A_{11} \\ \cdot \\ \cdot \\ \cdot \\ A_{ij} \end{bmatrix}, \tag{A4}$$

and the matrix of spatial functions is

$$[S] = \begin{bmatrix} S_{11}^1 & S_{12}^1 & S_{21}^1 & \vdots & S_{ij}^1 \\ S_{11}^2 & S_{12}^2 & S_{21}^2 & \vdots & S_{ij}^2 \\ S_{11}^3 & S_{12}^3 & S_{21}^3 & \vdots & S_{ij}^3 \\ \vdots & \vdots & \vdots & \vdots & \vdots \\ S_{11}^p & S_{12}^p & S_{21}^p & \vdots & S_{ij}^p \end{bmatrix}, \tag{A5}$$

where

$$S_{ij}^p = \sin(i\pi x_p/L_x) \sin(j\pi y_p/L_y). \tag{A6}$$

In the above equation, *i* and *j* represent the mode number. Each of the spatial coordinates of the randomly placed accelerometers are designated with (*x_p*, *y_p*), where *p* is the number of measurements taken. The modal accelerations were extracted by solving this system of linear equations. If measurements are taken such that the system is overdetermined, a least-mean-squares approach can be taken to solve for the desired modal amplitudes.

Since there are a finite number of measurements, spatial aliasing results. When nine measurements are made, only nine modal amplitudes can be resolved for a structure whose response is typically represented with an infinite number of modes. As a result, response of higher modes can “fold back” into the lower modes (i.e., the nine computed). When applying this technique, the response of the higher modes must be assumed negligible. This can be checked by observing the roll off in the amplitudes of the higher-order modes when included in the solution. To this end, the excitation frequency of the structure should be well below the resonant frequency of the highest mode which can be resolved.

Note that this method decomposes a system response into amplitudes or coefficients corresponding to the basis functions of Eq. (A6). For the open loop case, these basis functions correspond to the modes of the system. For the closed loop case, the system will have new mode shapes and resonant frequencies.¹⁷ However, it is convenient to decompose the closed loop response into the open loop modal components so that a direct comparison of the component changes can be made.

¹C. R. Fuller, “Active Control of Sound Transmission/Radiation from Elastic Plates by Vibration Inputs: I Analysis,” *J. Sound Vib.* **136**(1), 1–15 (1990).
²C. R. Fuller, R. J. Silcox, V. L. Metcalf, and D. E. Brown, “Experiments on Structural Control of Sound Transmitted Through an Elastic Plate,” in *Proceedings of American Control Conference*, Pittsburgh, PA (1989), pp. 2079–2084.
³C. H. Hansen, S. D. Snyder, and C. R. Fuller, “Noise Reduction of a Vibrating Square Panel by Use of Active Sound Sources and Active Vibration Sources: A Comparison,” in *Proceedings of Noise and Vibration 89*, Singapore (1989).
⁴E. F. Crawley and J. de Luis, “Use of Piezoelectric Actuators as Elements of Intelligent Structures,” *AIAA J.* **25** (10), 1373–1385 (1989).
⁵T. Bailey and J. E. Hubbard, “Distributed Piezoelectric-Polymer Active

- Vibration Control of a Cantilevered Beam," *AIAA J. Guidance Control* 6 (5), 605-611 (1985).
- ⁶J. L. Fanson and J. C. Chen, "Structural Control by the Use of Piezoelectric Active Members," in *Proceedings of NASA / DOD Control-Structures Interaction Conference*, NASA CP-2447, Part II (1986).
- ⁷B. T. Wang, E. K. Dimitriadis, and C. R. Fuller, "Active Control of Structurally Radiated Noise Using Multiple Piezoelectric Actuators," in *Proceedings of AIAA SDM Conference*, AIAA Paper 90-1172-CP, Long Beach, CA (1990).
- ⁸B. K. Wada, J. L. Fanson, and E. F. Crawley, "Adaptive Structures," *J. Intelligent Mater. Systems Struct.* 1 (2), 157-174 (1990).
- ⁹E. K. Dimitriadis and C. R. Fuller, "Investigation on Active Control of Sound Radiation from a Panel Using Piezoelectric Actuators," AIAA Paper No. 89-1062 (1989).
- ¹⁰C. R. Fuller, C. H. Hansen, and S. D. Snyder, "Active Control of Structurally Radiated Noise Using Piezoceramic Actuators," *Inter-Noise 89* 509-511 (1989).
- ¹¹R. L. Clark and C. R. Fuller, "Control of sound radiation with adaptive structures," *J. Intelligent Mater. Syst. Struct.* 2 (3), 431-452 (1991).
- ¹²J. Ochs and J. Snowdon, "Transmissibility Across Simply Supported Thin Plates, 1. Rectangular and Square Plates with and without Damping Layers," *J. Acoust. Soc. Am.* 58, 832-840 (1975).
- ¹³E. K. Dimitriadis, C. R. Fuller, and C. A. Rogers, "Piezoelectric Actuators for Distributed Vibration Excitation of Thin Plates," *J. Vib. Acoust.* 113(1), 100-107 (January, 1991).
- ¹⁴R. L. Clark, C. R. Fuller, and A. L. Wicks, "Characterization of Multiple Piezoelectric Actuators for Structural Excitation," *J. Acoust. Soc. Am.* 90, 346-357 (1991) (also presented at the 119th ASA meeting, April 1990).
- ¹⁵S. J. Elliott, I. M. Stothers, and P. A. Nelson, "A Multiple Error LMS Algorithm and its Application to the Active Control of Sound and Vibration," *IEEE Trans. Acoust. Speech Signal Process.* ASSP-35 (1), 1423-1434 (1987).
- ¹⁶B. Widrow and S. D. Stearns, *Adaptive Signal Processing* (Prentice-Hall, Englewood Cliffs, NJ, 1985).
- ¹⁷R. A. Burdisso and C. R. Fuller, "Theory of Feed Forward Control System Eigenproperties," *J. Sound Vib.* 153(3), 437-452 (1992).
- ¹⁸R. L. Clark and C. R. Fuller, "Modal Sensing of Efficient Acoustic Radiators with PVDF distributed Sensors in Active Structural Acoustic Approaches," *J. Acoust. Soc. Am.* 91, 3321-3329 (1992).